

Supporting Information

Unlocking Long-Term Stability in Metal-Based Gas Diffusion Electrodes for CO₂ Electoreduction

Chandani Singh^{1#}, Jia Song^{1#}, Ranjith Prasannachandran¹, Asier Grijalvo Rodriguez¹, Jing Shen¹, Zhiyuan Chen¹, Jan Vaes¹, Yuvraj Y. Birdja^{1}, Deepak Pant^{1,2*}*

¹ Electrochemistry Excellence Centre, Material and Chemistry (MatCh), Flemish Institute for Technological Research (VITO), Boeretang 200, 2400 Mol, Belgium

² Center for Advanced Process Technology for Urban Resource recovery (CAPTURE), Frieda Saeyssstraat 1, 9000 Gent, Belgium

[#]equal contribution

Contacts: yuvraj.birdja@vito.be; deepak.pant@vito.be

Table of contents

1. Experimental Section.....	2
1.1. Preparation of Metal GDE (Bi and Sn-GDE)	2
1.2. Electrochemical experimental setup	3
1.3. Activation of GDEs	4
1.4. Electrode characterization	6
1.4.1. Scanning electron microscope	6
1.4.2. Raman Spectroscopy	7
1.5. Product analysis.....	7
2. Electrochemical experiments.....	8
2.1. Sn and Bi GDE	8

1. Experimental Section

1.1. Preparation of Metal GDE (Bi and Sn-GDE)

Tin powder (99.8%, 325 mesh, Alfa Aesar), Bismuth powder (99.5%, 325 mesh size, Thermo Scientific Chemicals), PTFE (DuPont™ 669N X), ammonium bicarbonate (ambic), NH_4HCO_3 (98%, ACROS Organics), potassium bicarbonate (from Acros Organics Extra) and potassium hydroxide pellets (KOH, Ensure), were used as purchased. For electrochemical experiments, flow cell from ElectroCell® with a geometrical area of 10 cm^2 was used along with Nafion 115 and Fumasep® FBM (Bipolar membrane) as specified in the electrochemical setup (vide infra). A mass flow controller, peristaltic pump and mass flow meter BPC GO® (as a volumetric flow for the outlet of the cell) were used.

Sn-GDE and Bi GDE were prepared by following the protocol as reported in the patent filed by VITO in 2021.^[1] A layer-by-layer approach was implemented for the manufacturing of the GDE which includes separately preparing the gas diffusion layer (GDL) and catalyst layer (CL). The GDL consists of PTFE (DuPont™, 669N X) as a binder and ammonium bicarbonate (ambic) as a pore former mixed in the weight ratio of 70:30. The catalyst layer (CL) consists of metal powder (Sn and Bi respectively), mixed with PTFE and ambic in the weight ratio of 70:20:10. Both layers were prepared as a $10\times 10\text{ cm}^2$ cake using the hydraulic press and then cold rolled into a thin sheet of GDL and CL with the thickness of 0.4 - 0.5 mm each. Both layers were combined in the final stage to create a single sheet containing GDL and

CL with a final thickness of 0.4 - 0.5 mm. The so formed layers were kept in an oven at 70 °C for 6 h allowing the ambic to evaporate forming a porous metal GDE. The Sn-GDE needs to be electrochemically activated before its implementation in ECR. The activation process of Sn-GDE is discussed in detail in the result and discussion section.

1.2. Electrochemical experimental setup

All electrochemical experiments were carried out using VSP BioLogic potentiostat clubbed with VMP3 BioLogic current booster and EA-PS 2042-10 bench-top programmable power supply (42V, 10A ,160W), EA Elektro-Automatik. ElectroCell® microflow cell with an effective geometrical area of working electrode as 10 cm² was used as electrochemical cell. The metal GDE (Sn and Bi GDEs) as working electrode, LF-1-100, Ag/AgCl as reference electrode and dimensionally stable anode (DSA) composed of mixed metal oxides of Ir and Ru as counter electrode. Unless otherwise specified 0.5 M KHCO₃, 5 L, saturated with CO₂, was used as catholyte and 3 M KOH, 2 L, as anolyte. The cell assembly is illustrated in figure S1. The microflow cell comprised a gas chamber facing the GDL side of the GDE, followed by the GDE, catholyte chamber with CL towards one side and membrane on the other. Following the membrane the anolyte chamber followed by anode plate (DSA). The reference electrode, LF-1-100, Ag/AgCl, was inserted between the catholyte and membrane layer. The cell was assembled with a Fumasep® FBM bipolar membrane in a reverse bias mode. During the experiment, 30 mL/min flow of CO₂ was used, controlled by BROOKS® mass flow controller. Electrolytes were circulated in the cell using a peristaltic pump of Verse with a 60 mL/min flow.

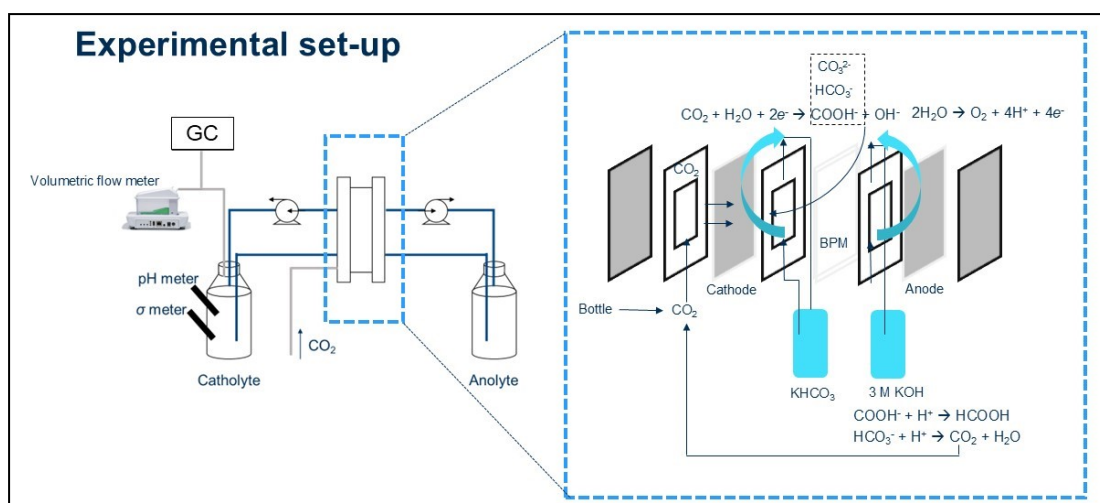


Figure S1. Electrochemical CO₂ reduction set-up utilized for the long-term experiments.

The flow-through mode of operation was used for the experiment. In a flow through mode of operation, the gas is forced to pass through the GDE, and all the gas products are collected at the catholyte reservoir. The gas collected is analysed with on-line headspace gas-chromatogram. Prior to each electrochemical experiment, the catholyte (0.5 M KHCO_3) was saturated with CO_2 overnight (6-8 h). BPC Go[®], a flow meter, was used at the outlet of cell to monitor the exit flow of gas from the cell. To maintain identical reaction conditions, said current was applied only reaching a stable signal from outlet of the electrochemical cell (EC) for CO_2 by BPC Go[®] flowmeter (when inlet CO_2 flow is equal to outlet CO_2 flow). This ensured an identical reaction condition regarding gas species equilibrium, pH and catholyte conductance before the experiment's commencement. All reported electrode potentials are referenced to Ag/AgCl (3 M KCl) unless otherwise stated. Potentials were not converted to the RHE scale because the pH varied during operation, making accurate correction unreliable.

1.3. Activation of GDEs

The GDEs (Sn and Bi GDE) require an electrochemical sintering step, known as the activation step, before any electrocatalytic process can begin.^[1-2] The manufacturing process for the GDEs does not involve external current collectors, and the subsequent application of a PTFE layer for hydrophobic GDL results in high in-plane resistance. The activation step serves to sinter the electrodes, reducing the in-plane resistance from 1-10 $\text{M}\Omega \text{ cm}^{-2}$ to 0.2-0.8 $\Omega \text{ cm}^{-2}$. High current density (400-500 mA cm^{-2}) is passed through the electrodes to activate them, leading to the formation of thin metallic layers and a decrease in in-plate resistance to $< 1 \Omega \text{ cm}^{-2}$ (0.2-0.8 $\Omega \text{ cm}^{-2}$). The changes in the surface of the GDE before and after activation are clearly visible in SEM images (Figure S2, Supporting Information - before and after activation).

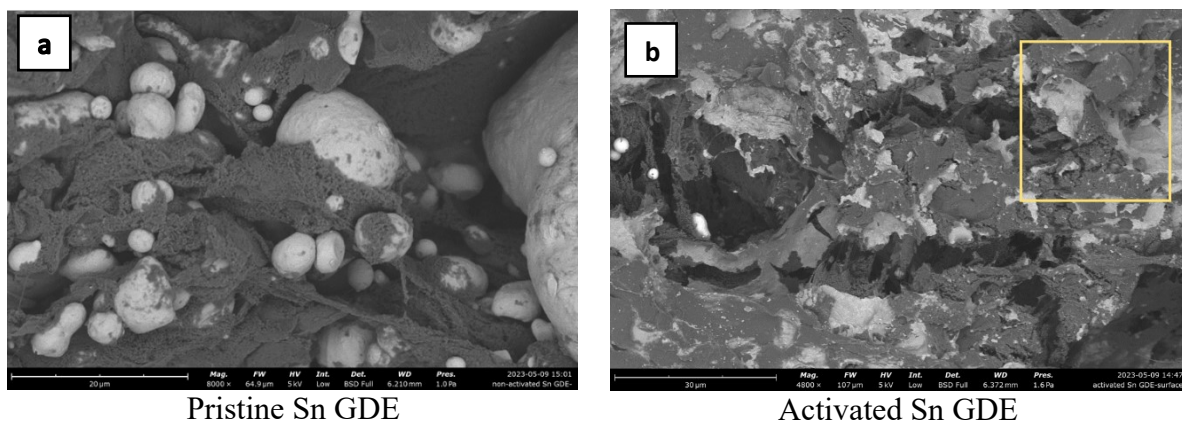


Figure S2. SEM images of (a) pristine Sn GDE and (b) freshly activated Sn GDE. The light grey represents Sn, and the black part represents PTFE. The yellow box highlights the portion containing both Sn and PTFE region represented by light grey and dark grey colour.

The comparison of the SEM images of the pristine and freshly activated GDEs offers valuable insights into the surface changes that occur during the activation process. The SEM images clearly show that the pristine GDE displays segregated Sn/Bi particles dispersed throughout the PTFE binder. The high resistance of these GDEs can be attributed to the poor interconnectivity between these segregated metal islands (see figure S2, S3). However, the activation process leads to electrochemical sintering, which connects these segregated metal islands with a thin film of metal layer (Sn and Bi, respectively), decreasing the planar resistance of the electrodes. This is also supported by the LSV scan of the Sn GDE (figure S4).

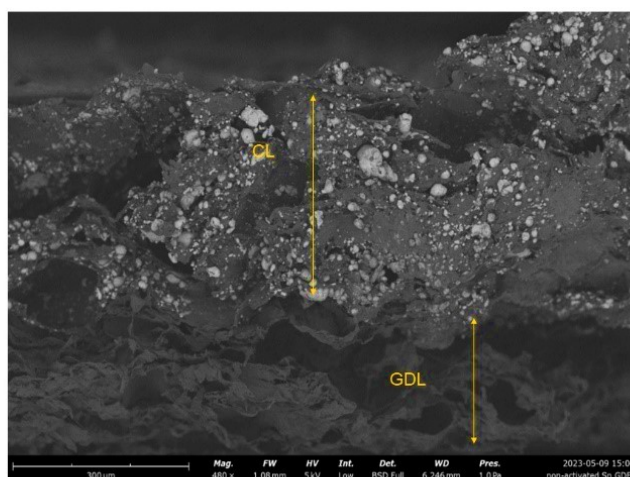


Figure S3. Cross-section SEM image of pristine Sn GDE depicting clear distinction between the GDL and CL.

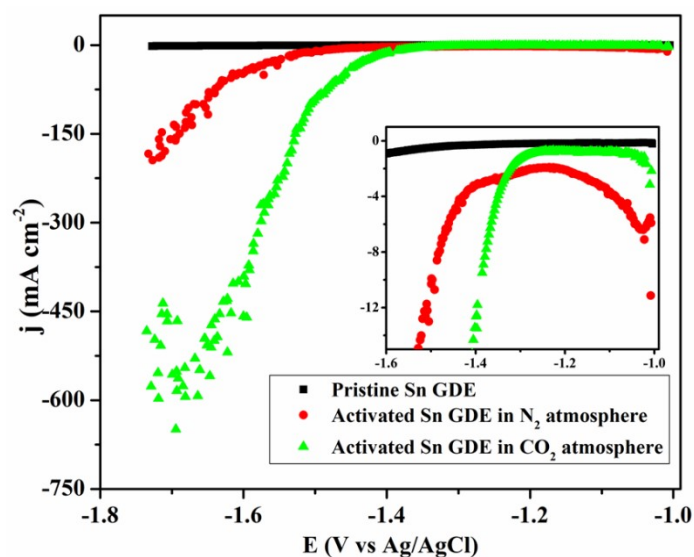


Figure S4. Linear sweep voltammetry (LSV) of Sn GDE before and after electrochemical activation under N₂ and CO₂ atmospheres (inset highlighting the lower current density range for clarity). The higher current density observed post-activation confirms enhanced electrode conductivity and improved electrical connectivity within the GDE structure.

1.4. Electrode characterization

Morphological changes in the electrodes were analyzed before and after electrochemical testing. These were analyzed by SEM and in situ Raman spectroscopy. For SEM analysis, the electrodes were cleaned by dipping them in DI water for a few minutes to remove excess salt deposition from electrolyte exposure, then drying them in dry air. A small part of the electrode was cut and used directly for the SEM analysis.

1.4.1. Scanning electron microscope

Scanning electron microscope (SEM) images were taken using Phenom ProX Desktop SEM designed by Thermo Fischer Scientific. It is equipped with a long-lifetime CeB6 source and integrates SEM and EDS functions into a single interface. It has a light optical magnification of 27-160x and an electron optical magnification range of 160-350000x. It offers a resolution of 6 nm SED and 8 nm BSD. The accelerator voltages can be adjusted between 5kV and 15kV (4.8kV and 20.5kV in the advanced mode), and it can accommodate a sample size of up to 25 mm in diameter (optional 32 mm) and up to 35 mm in height (optional 100 mm).

1.4.2. Raman Spectroscopy

Raman spectroscopic analyses were conducted using a confocal Raman microscope (Renishaw InVia) with WiRE5.3 data processing software. The calibration was performed using a silicon wafer standard at 521 cm^{-1} . A 532 nm laser served as the excitation source, and the incident beam was attenuated to 10% of its initial power for measurements. Raman spectra were collected in the range of 100 to 3000 cm^{-1} . The counter electrode consisted of a Pt coil, and the reference electrode was an Ag/AgCl electrode immersed in a saturated KCl solution. The working electrode was a $0.2\text{ cm} \times 0.2\text{ cm}$ Bi-metal electrode. An electrochemical potentiostat (PalmSens) was utilized to control and measure potentials and currents.

The electrochemical setup utilized for *in-situ* Raman spectroscopy had CO_2 -saturated 0.5 M KHCO_3 electrolyte in a three-electrode cell (Dek Research Instrumentation). The experiments mimicked the conditions applied to the Bi-GDEs flow cell experiments. Briefly, H-type *in-situ* Raman spectroscopy cell with a single light window from Dek Research Instrumentation was used. 0.5 M KHCO_3 and 1 M KOH were used as catholyte and anolyte respectively, separated by Nafion 117 membrane. A $0.2\text{ cm} \times 0.2\text{ cm}$ Bi foil was used as the cathode. The experiment was designed to gain insight in the reactivation process and to identify the key species involved.

1.5. Product analysis

Both liquid and gas samples were analysed periodically during the operational duration of the electrolyser. Liquid products were manually taken out (1 ml) from both anolyte and catholyte at a fixed interval of few hours. The collected liquid samples were subsequently analysed by High-Performance Liquid Chromatography (HPLC). Agilent 1200 HPLC equipped with an Agilent Hi-Plex H $7.7 \times 300\text{ mm}$ column was used to separate the product. Agilent 1260 RID detector was employed to detect and quantify the formate in the form of formic acid. Prior to the analysis, the samples were previously diluted with water and acidified with H_2SO_4 to prevent bubble formation and column obstruction. $0.01\text{ M H}_2\text{SO}_4$ was used as the mobile phase.

Gas-phase products from the electrochemical cell were measured using online Gas chromatography (GC). Interscience Compact GC equipped with three analytical columns: ShinCarbon ST, Haysep N, and Molsieve 5. These columns facilitated the separation of permanent gases and hydrocarbons. Helium was used as the carrier gas for the ShinCarbon ST

and Haysep N columns, while Argon was used for the Molsieve 5A column to enable efficient separation and thermal conductivity detection of hydrogen. Gas detection was performed using both a thermal conductivity detector (TCD) and a flame ionisation detector (FID).

For total Faradaic efficiency determination, gas-phase (GC) and liquid-phase (HPLC) data were combined without normalization to 100%. Formate concentration in the anolyte was included in the total FE accounting to crossover correction.

2. Electrochemical experiments

2.1. Sn and Bi GDE

All the electrochemical experiments were performed as mentioned in Section 1.2. Figure S5 represents the long-term experiment with Sn GDE.

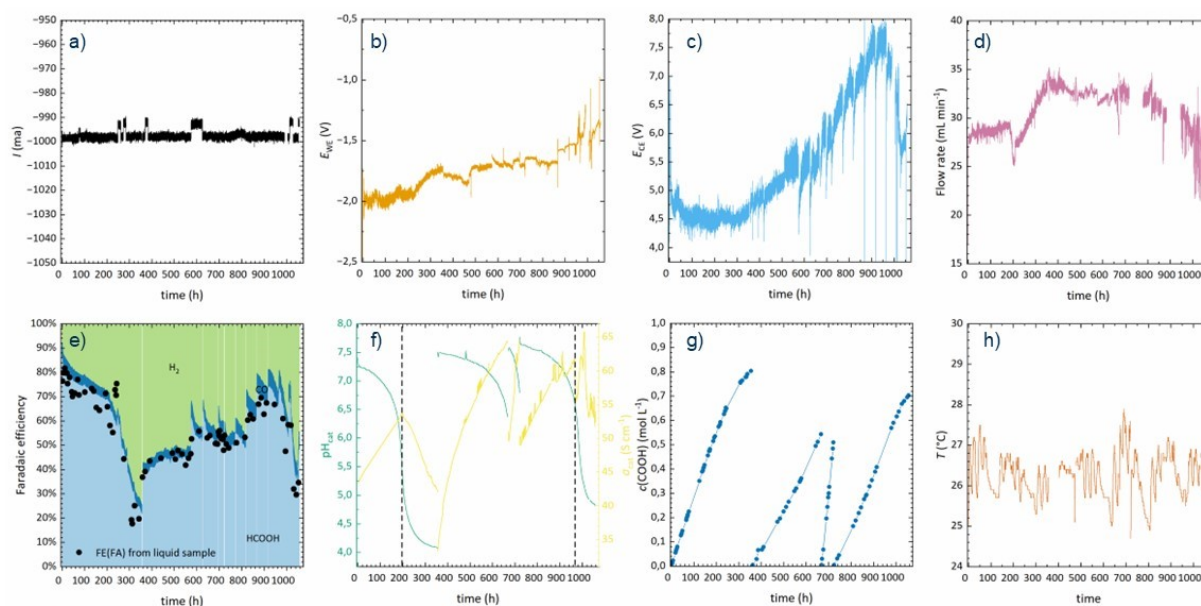


Figure S5. The changes in (a) applied current, (b) working potential (E vs. Ag/AgCl), (c) counter electrode potential (E vs. Ag/AgCl), (d) outlet flow of gases from the outlet of the electrochemical cell, (e) Faradaic efficiency of formate/formic acid, H_2 and CO , (f) pH and conductance of the catholyte, (g) concentration of formate accumulated in the catholyte, and (h) applied current during the long-term experiment with Sn GDE.

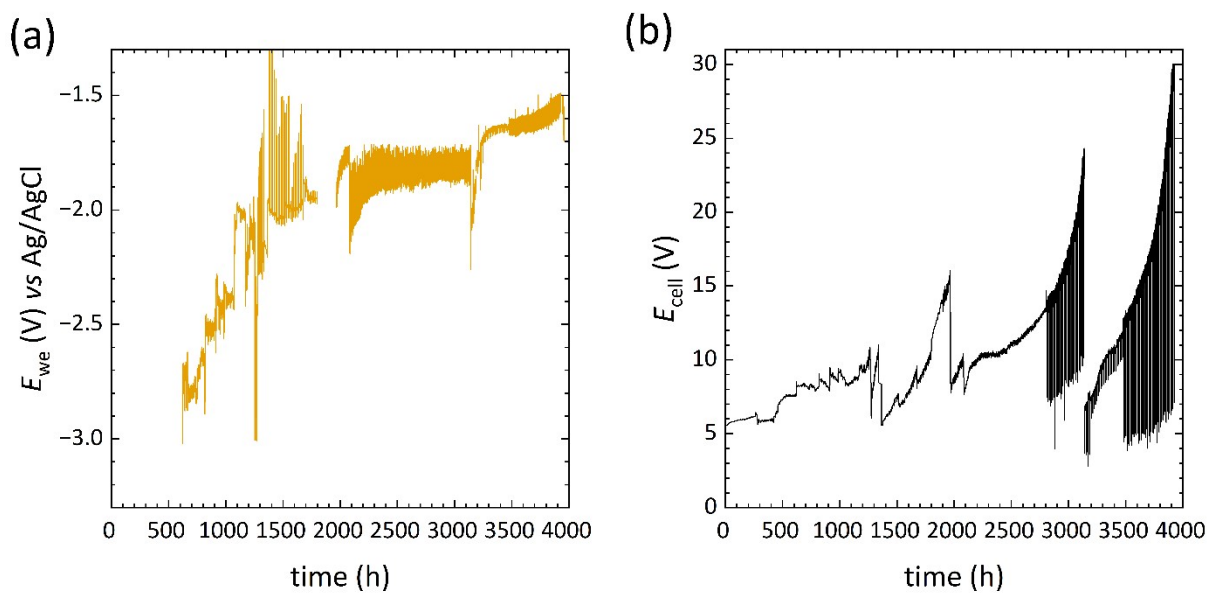


Figure S6. Bi GDE operated at 100 mA cm^{-2} : (a) working-electrode potential, E_{we} vs. Ag/AgCl, as a function of time, and (b) corresponding cell voltage, E_{cell} . The gradual drift to more negative potential and higher cell voltages correlates with the degradation and reactivation zones discussed in the manuscript. The strong increase in cell voltage at $t > 3000 \text{ h}$ is caused by failure/clogging of the membrane leading to high membrane resistance.

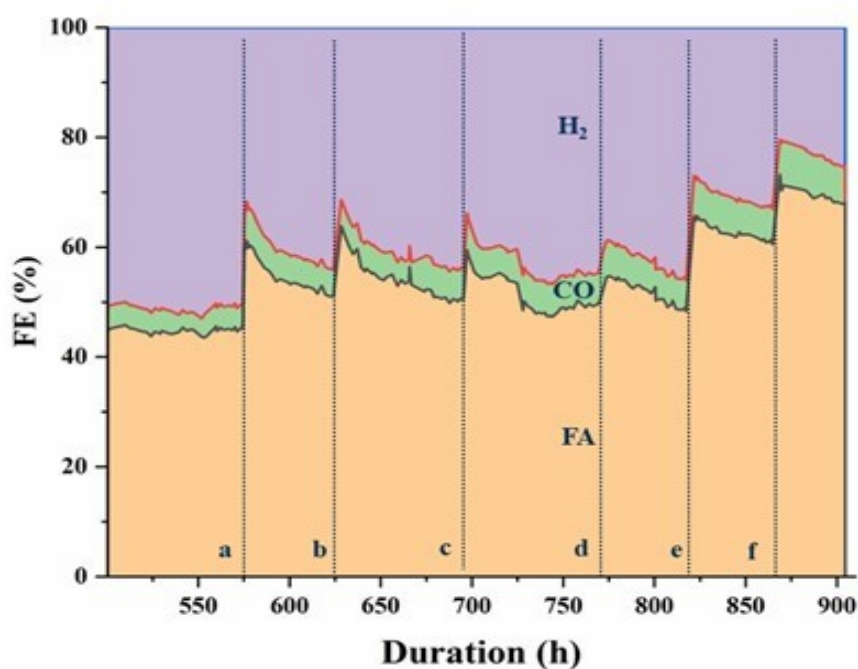


Figure S7. Sn GDE in reactivation zone, slowly increasing the formate (FA) FE from 40% to 65%. The dotted lines indicate when anodic pulsing was applied.

The reactivation was first evaluated by applying an anodic potential pulse of +2 V for 30 s (Figure S7, markers a and b). The protocol was subsequently refined to galvanostatic

anodic pulses of 0.5 A for 30 s, applied at varying pulsing frequencies (Fig. S7c–f), with the corresponding parameters summarised in Table S2.

Under the initial pulsing conditions, the FE_{FA} increased from 46% to 62%, followed by a progressive decrease to $\sim 50\%$ prior to the next pulse. The irregularity in the frequency at which the electrode was induced was due to looking into the degradation of the catalytic properties of the catalyst, once it is subjected to pulse. As evident from the later pulsing stage (d-f), more frequent pulsing helped in sustaining the catalytic activity. These observations indicate that increasing the pulsing frequency can more effectively sustain the FE_{FA} , in agreement with the performance trends shown in Fig. 4 of the main manuscript.

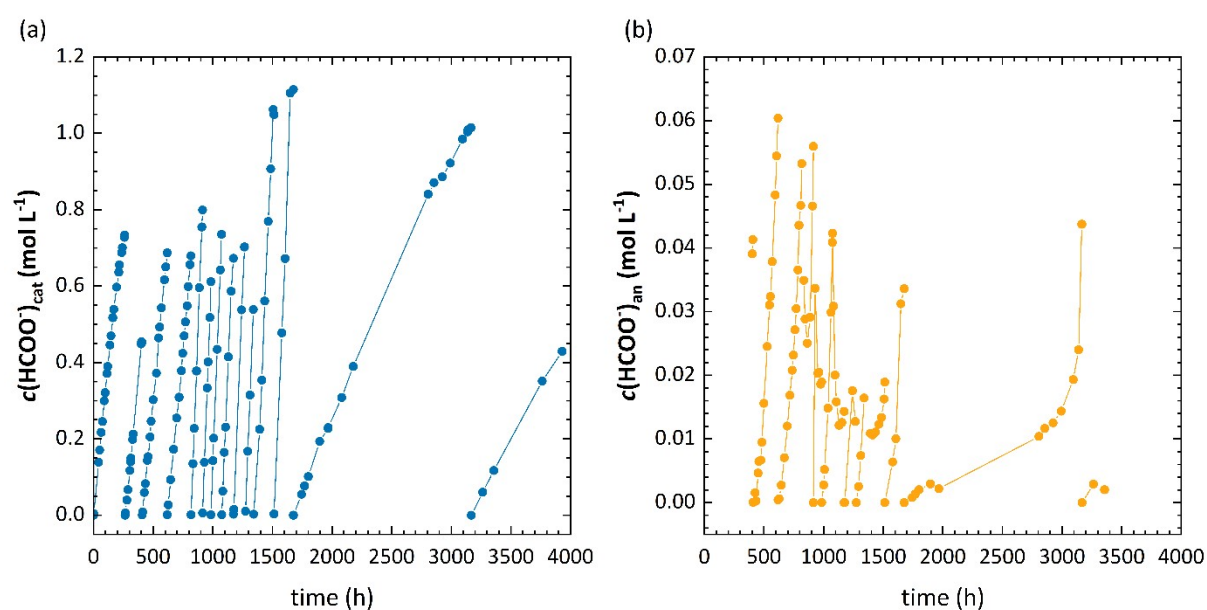


Figure S8. Long-term evolution of formate concentration during Bi-GDE operation at 100 mA cm⁻². (a) Formate concentration in the catholyte, showing continuous accumulation throughout the electrolysis. (b) Formate concentration in the anolyte, demonstrating proportional crossover of formate through the bipolar membrane.

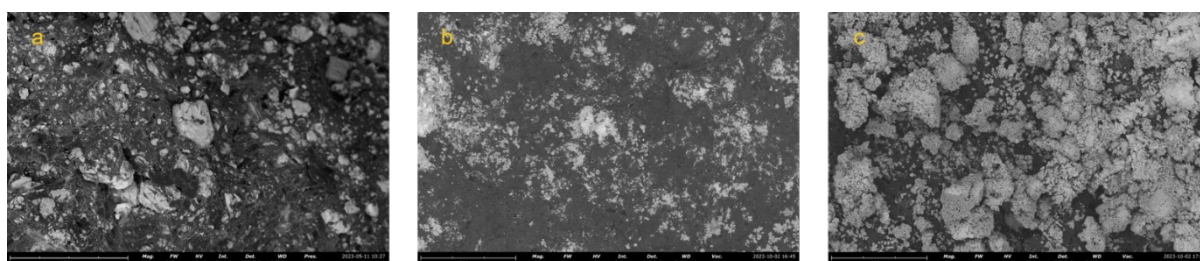


Figure S9. SEM images of (a) pristine Bi GDE, (b) Bi GDE after 4000 hours, with little Bi coverage, and (c) Bi GDE after 4000 hours, with Bi coverage.

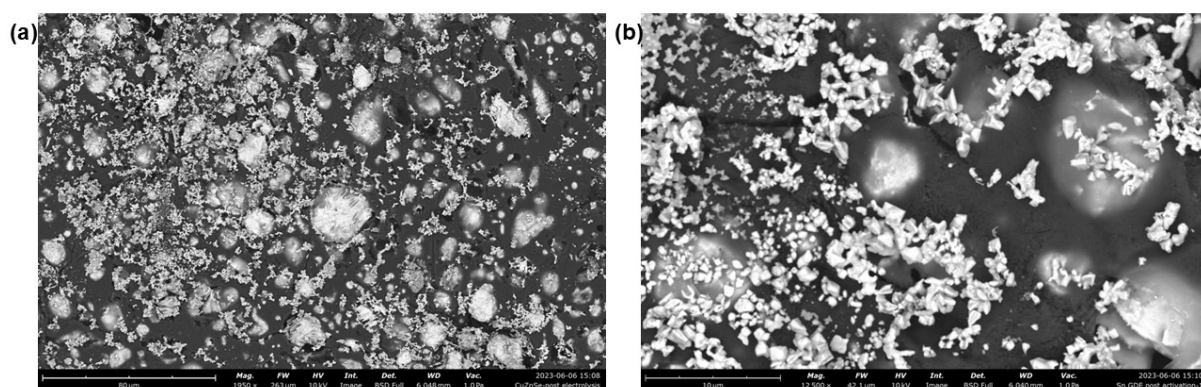


Figure S10. SEM images of Sn GDE after 1000 hours in different resolutions: (a) 150 mm scale and (b) 10 mm scale.

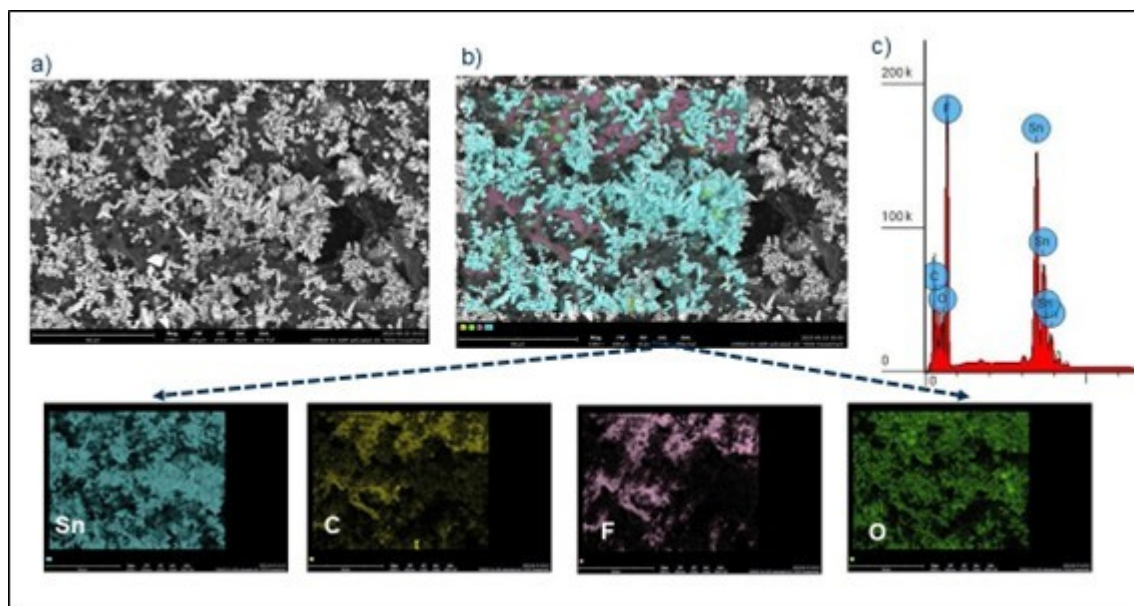


Figure S11. SEM and EDS analysis of the Sn GDE after 1000 h of electrolysis. (a) SEM image showing the overall surface morphology; (b) EDS mapping of Sn GDE showing different element present on the morphology. Elemental maps for Sn, C, F, and O are shown below, indicating the spatial distribution of tin, carbon, fluorine, and oxygen on the electrode surface after extended operation. (c) corresponding EDS spectra.

Table S1. Data of sampling time, FA concentration, catholyte volume and calculated FE_{FA} of the liquid samples taken in the first 260 hours.

Sampling time (h)	FA concentration (M)	Catholyte volume (mL)	Calculated FE_{FA}
0.00	0.0000	5000	
1.30	0.0040	4997	83.08%
42.95	0.1392	4944	85.95%
50.47	0.1709	4933	89.69%
64.44	0.2172	4915	86.24%
73.15	0.2458	4903	84.61%
89.90	0.2996	4880	82.18%
96.50	0.3212	4871	83.53%
112.29	0.3711	4850	79.83%
119.42	0.3897	4840	64.74%
137.75	0.4462	4816	76.93%
145.77	0.4696	4805	71.62%
161.84	0.5174	4784	73.05%
169.47	0.5391	4773	68.92%
192.69	0.5972	4743	59.80%
211.17	0.6364	4718	49.50%
216.90	0.6557	4710	80.00%
234.20	0.6878	4687	41.91%
240.75	0.7004	4678	43.08%
257.30	0.7278	4656	36.43%
261.36	0.7336	4650	29.57%

Table S2. Summary of pulsing conditions applied during the electrolysis experiment with Sn GDE. The “Operational Time” indicates the cumulative running time of the experiment at which each anodic pulse was introduced. Pulses were applied in either potentiostatic (+2.0 V vs. Ag/AgCl) or galvanostatic (0.5 A) mode, with the specified duration, to probe the effect of pulse type and frequency on formate selectivity.

Pulse label	Operational time	Mode of pulse	Condition	Duration of pulse
a	575	Potentiostatic	+ 2 V vs. Ag/AgCl	60
b	625	Potentiostatic	+ 2 V vs. Ag/AgCl	60
c	690	Galvanostatic	0.5 A	60
d	770	Galvanostatic	0.5 A	30
e	820	Galvanostatic	0.5 A	30
f	820	Galvanostatic	0.5 A	30

References

1. Jacobs, B.; Pant, D.; Van Houtven, D.; Maes, E.; Vaes, J.; Birdja, Y. Y. Carbon-Free Gas Diffusion Electrode. European Patent **EP 4182491 B1**, granted 2 July 2025.
2. Singh, C., Song, J., Radomski, J., Chen, Z., Birdja, Y. Y., Vaes, J. and Pant, D. Re-activation process of gas diffusion electrode, *European patent application*, 2024, **EP4474526A1**.